An Analysis of Juno Downlink Ka-band Carrier Data

David D. Morabito,* Dustin Buccino,* and Daniel Kahan*

ABSTRACT. — Ka-band downlink data from the Juno spacecraft were analyzed in order to characterize the performance of carrier signal-to-noise density ratio measurements relative to expected link budget performance. Data were acquired from the three DSN tracking sites (Goldstone, Canberra, and Madrid) between 2013 and 2023. Anomalous observations, defined as those below an adverse link budget minus an additional 4 dB, were itemized by stations, sites, and years; and furthermore, characterized by correlating with event data from monitor data (e.g., weather) and Juno radio science reports. The Juno Ka-band statistics were integrated with those derived from previous studies involving the Cassini, Kepler, and MRO spacecraft Ka-band downlinks. Such statistics are useful to future missions that may be considering incorporating a Ka-band downlink on their spacecraft.

I. Introduction

Ka-band (32 GHz) offers several advantages over lower frequency bands, such as wider spectrum allocation, higher antenna gain, and greater immunity to plasma effects. These advantages facilitate increased telemetry performance and greater accuracy for differential one-way ranging (DOR), Doppler, and ranging navigation data types. Early deep-space Ka-band experiments and demonstration flights included Mars Observer, Mars Global Surveyor, Deep Space 1, and Mars Reconnaissance Orbiter (MRO). Ka-band (32 GHz) and K-band (26 GHz) missions whose downlink signal strength data have been analyzed include Cassini [1], Kepler [2], MRO [3], and Lunar Reconnaissance Orbiter (LRO) [4–5]. In addition, telemetry frame errors from the Kepler Ka-band data sets were analyzed [6]. The focus of this study is on examining Ka-band carrier data from Juno's radio science investigation (to date) in the context of performing a statistical analysis in the same manner as was done previously for Cassini, Kepler and MRO. These results are integrated into the overall Ka-band statistical database.

II. Observations and Results

This section summarizes the statistical results of Juno Ka-band carrier-to-noise density (P_c/N_0) measurements acquired by the DSN closed-loop receivers at Goldstone, California

* Communications Architectures and Research Section.

The research described in this publication was carried out by the Jet Propulsion Laboratory, California Institute of Technology, under a contract with the National Aeronautics and Space Administration.

(Section II.A); Canberra, Australia (Section II.B); and Madrid, Spain (Section II.C). The measurements are adjusted to a common range distance of 9.62×10^8 km (6.43 AU) to allow for easy inter-comparisons between tracks. The measurements are then plotted as a function of elevation angle along with the Favorable and Adverse link curves for each site.

We make use of percent weather statistics of atmospheric attenuation and atmospheric noise temperature increase for the link curves as documented in the DSN 810-005 module on "Atmospheric and Environmental Effects" [7]. For the Favorable weather link curve, we assume 0% weather and for the Adverse weather link curve, we assume 95% weather. In addition, we assume no Jupiter hotbody noise for the Favorable link curve, and a maximum Jupiter hotbody noise of 14 K for the Adverse link curve. We also assume a worst-case pointing loss of 2 dB for the Adverse link curve. The link models also make use of elevation dependent models for ground station antenna gain and noise temperature for the DSN 34-m beam waveguide antennas [8].

We also plot an additional curve, called "Adverse – 4 dB" link curve (4 dB lower than the Adverse case defined above) in order to examine the number of P_c/N_0 measurements that lie below it. The data tables provided in this report show the total number of P_c/N_0 measurements, the total number of "valid" P_c/N_0 measurements, the total number of measurements that lie above the Adverse – 4 dB link curve, and the percent of valid measurements that lie above the Adverse – 4 dB link curve. "Valid" measurements involve those after "Invalid" or "Bad" data points were removed from the data sets for various reasons. Among these invalid points were those due to injected calibration signals prior to (i.e., during pre-cal time) or after (i.e., during post-cal time) the tracks.

A. Goldstone

This section summarizes the statistical results of Juno Ka-band carrier-to-noise density (P_c/N_0) measurements acquired by the DSN closed-loop receivers at Goldstone, California. A majority of Ka-band data for Juno are collected at DSS-25, due to the presence of the Ka-band transmitter at the station. There are about 2.74 million total observations and about 2.69 million observations after removing those affected by injected signals during calibrations.

Table 1 summarizes the Juno Ka-band carrier data that were acquired by the closed-loop receivers at the 34-m antenna designated DSS-25 (Table 1a) and DSS-26 (Table 1b) as well as the Goldstone composite totals (Table 1c). Each table displays the year of the observations, the total number of data points, the number of valid observations (displayed in Figure 1 after removal of known "invalid" or "bad" points), number of data points lying above the Adverse – 4 dB curve and the percentage of valid data points lying above the Adverse – 4 dB curve. About 99% of the data lie above the Adverse – 4 dB curve for DSS-25 and about 88% for DSS-26, with a net value of 98% for the composite case. The overall total 88 percent of data lying above the Adverse – 4 dB curve for DSS-26 is heavily skewed by the very low 46% value for year 2015, for which details are provided below.

Table I. Summary of Juno Ka-band Carrier Observations Acquired at Goldstone

Table 1a – Goldstone DSS-25

Year	Number of Total Obs	Number of Valid Obs	Number Obs > Adv. – 4 dB	Percent > Adv. – 4 dB
2013	135,511	130,009	128,639	98.946
2015	226,351	224,879	224,745	99.940
2016	117,188	113,497	112,553	99.168
2017	286,113	283,980	283,319	99.767
2018	257,817	253,781	253,267	99.797
2019	293,052	291,531	273,952	93.970
2020	391,518	382,341	380,044	99.399
2021	269,188	265,262	264,256	99.621
2022	276,449	272,773	271,448	99.514
2023	333,237	328,362	326,325	99.380
Total	**2,586,424**	**2,546,415**	**2,518,548**	**98.91**

Table 1b – Goldstone DSS-26

Year	Number of Total Obs	Number of Valid Obs	Number Obs > Adv. – 4 dB	Percent > Adv. – 4 dB
2015	32,398	31,934	14,658	45.901
2018	91,673	91,267	91,008	99.716
2019	25,560	24,605	24,592	99.947
Total	**149,631**	**147,806**	**130,258**	**88.13**

Table 1c – Goldstone Totals

Station	Number of Total Obs	Number of Valid Obs	Number Obs > Adv. – 4 dB	Percent > Adv. – 4 dB
DSS-25	2,586,424	2,546,415	2,518,548	98.906
DSS-26	149,631	147,806	130,258	88.128
Total	**2,736,055**	**2,694,221**	**2,648,806**	**98.31**

1. Goldstone DSS-25 Ka-band Observations

This section summarizes the statistical results of closed-loop receiver observations of Juno Ka-band carrier data acquired at DSS-25. Figures 1a through 1j display the individual adjusted P_c/N_0 data points (in blue) for years 2013 to 2023. Also shown are the Favorable link curve (solid black), the Adverse link curve (solid red), and the Adverse – 4 dB link curve (dashed yellow). As expected, the vast majority of the data points lie in between the Favorable and Adverse link curves, as well having the top of the envelope of the blue data points align up against the Favorable link curve.

Figure 1a displays the adjusted Ka-band P_c/N_0 for year 2013 where we see a "snowfall" effect of data points lying below the Adverse – 4 dB curve. Such behavior has been attributed to high winds in previous data sets, which is also true in Juno's case. The higher frequency Ka-band link is more susceptible to high winds due to its smaller beam size than the lower frequency X-band link. During data collection, the Juno radio science team correlated numerous power drops with high-wind events. High-profile examples of weather affecting the data occurred in November 2020, September 2022, and March 2023, though additional events throughout the mission did occur as demonstrated in the examples below. Anomalies in the Antenna Pointing and Control (APC) system at the station could also introduce very low P_c/N_0 readings since, in such cases, the DSN antenna would not be optimally pointed. Additionally, 30 minutes after each acquisition by the closed-loop receiver, a monopulse on-point phase calibration is performed in which a small offset is manually introduced to the antenna pointing, reducing Ka-band received power by 3–6 dB. These calibrations are used to calibrate the monopulse pointing system [9]. This special procedure was implemented into normal Ka-band tracks for Juno to avoid the need for separate calibration tracks.

Figure 1e displays adjusted P_c/N_0 versus elevation angle for year 2018, which for the most part shows nominal behavior.

Figure 1f displays adjusted P_c/N_0 versus elevation angle for year 2019, which appears to contain some non-standard passes. There were "problematic" or "non-standard" signatures seen in three of the 2019 tracks, one on 2019-112 (Figure 2), one on 2019-254 (Figure 3) and one on 2019-238 (Figure 4a). An expanded view of the adjusted P_c/N_0 for pass 2019-238 (Figure 4b) shows a periodic variation of about 31 seconds.

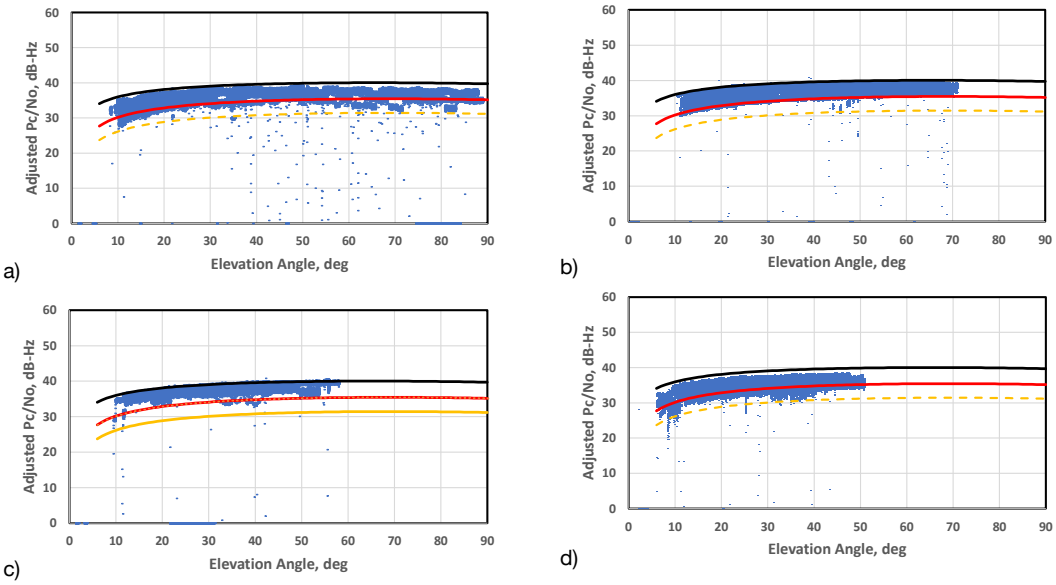

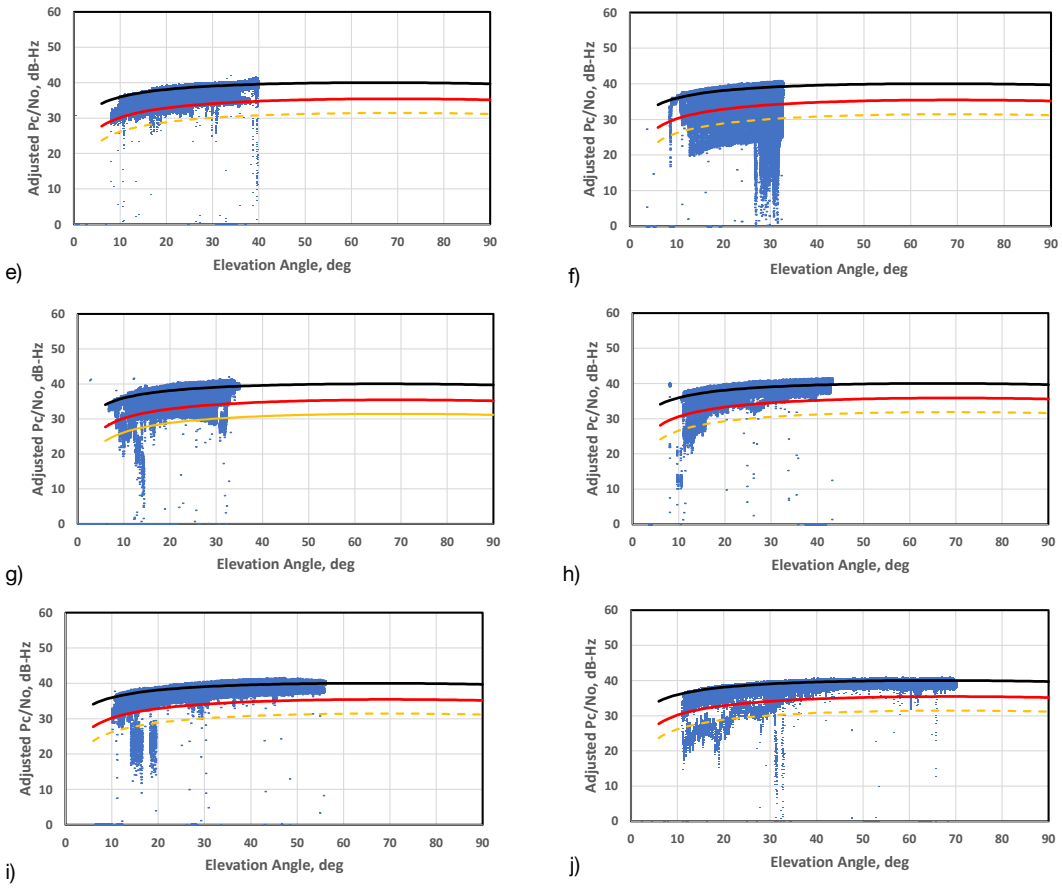

Figure 1. Adjusted Ka-band P_c/N_0 versus elevation angle (blue) from DSS-25 for year a) 2013, b) 2015, c) 2016, d 2017, e) 2018, f) 2019, g) 2020, h) 2021, i) 2022, and j) 2023. Also shown are the favorable (black), adverse (red) and "Adverse – 4 dB" (dashed yellow) link curves.

On 2019-112, the monopulse pointing system used by the DSN failed and introduced invalid pointing commands to the antenna, driving it off-point (Figure 2).

On 2019-254/255, high winds were noted by radio science staff during the first half of the tracking pass (Figure 3).

On 2019-238, the spacecraft's High Gain Antenna (HGA) was not optimally pointed towards Earth (Figure 4a). Based on the beam pattern of Juno's HGA, the signal power would be reduced by approximately 10 dB and introduce a spin signature in the power and Doppler measurements, caused by Juno's spin rate at 2 rotations-per-minute (see Figure 4b).

Figure 1g displays the adjusted P_c/N_0 versus elevation angle for year 2020 where we see some low value data points. The features in the 2020-312/313 (Nov 7–8) data (Figure 5) that lie below the Adverse curve (see Figure 1g), involved severe weather, which not only caused issues with the link, but also affected the DSN pointing system's ability to function correctly (the monopulse pointing system failed to operate under the wind and rain conditions).

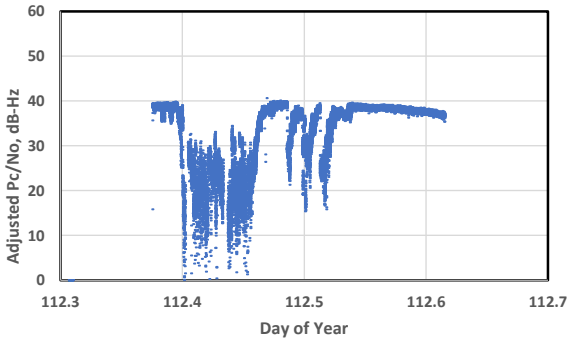

Figure 2. Adjusted P_C/N_0 versus Day of Year for pass 2019-112.

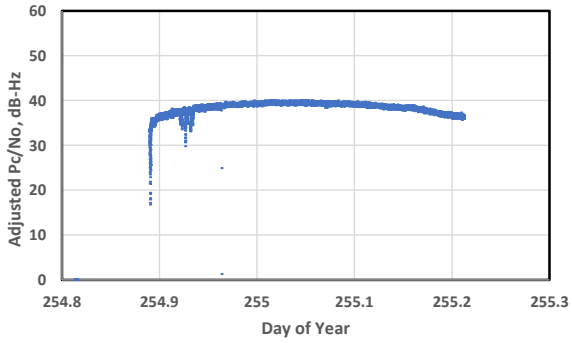

Figure 3. P_C/N_0 (adjusted) versus Day of Year for pass 2019-254/255.

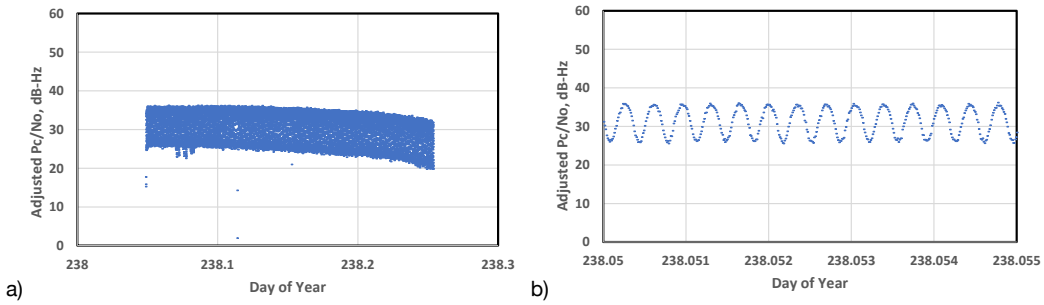

Figure 4. (a) Adjusted P_C/N_0 versus Day of Year for 2019-238. (b) Expanded view of Adjusted P_C/N_0 versus Day of Year for 2019-238.

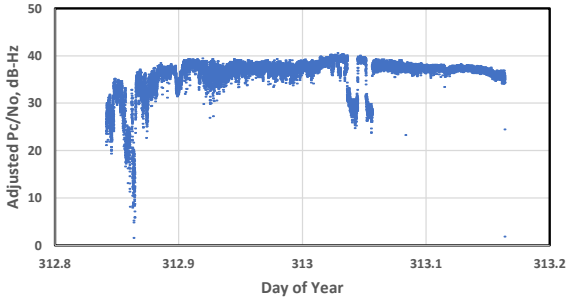

Figure 5. Adjusted P_C/N_0 versus Day of Year for 2020-312.

Figure 1h displays the adjusted P_c/N_0 versus elevation angle for year 2021, where there are also some low data points (to be investigated). Figure 6 displays adjusted P_c/N_0 versus time for pass 2021-189, where we see high scatter and drop-offs at start-of and end-of pass with interesting signatures caused by the monopulse pointing system unable to function, thus preventing optimal pointing for Ka-band reception. It was not possible to examine against system noise temperature (SNT) since the SNT reading was disabled during this pass.

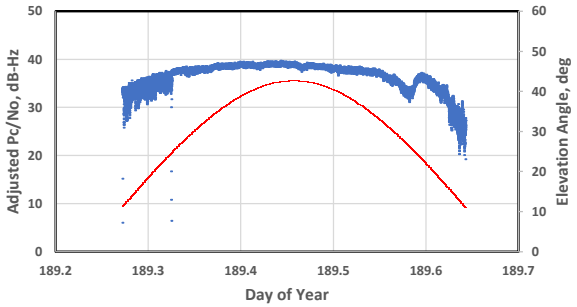

Figure 6. Adjusted P_C/N_0 (blue) and elevation angle (red) versus Day of Year for 2021-189.

Figure 1i displays adjusted P_c/N_0 versus elevation angle for year 2022, where we see some data points with low P_c/N_0 values clustered below 30 dB-Hz lying between ~14 to ~20 deg elevation angle. These occurred during pass 2022-041/042 and could be due to an issue with the monopulse or spacecraft antenna pointing.

Figure 1j displays adjusted P_c/N_0 versus elevation angle for year 2023, which shows nominal behavior, except for one pass which appears to have a possible rain issue.

Figure 7 displays the adjusted P_c/N_0 versus time for pass 2023-250, which appears to have suffered a rain event near the end of the pass. The retrieved rain gauge data from the on-site weather sensors do indeed show that significant rainfall events occurred at that time period (at 16:36 and 16:42 UTC).

Figure 8 displays the adjusted P_c/N_0 and elevation angle versus time where signal dropouts were seen on 2023-212 between 09:49 and 09:59 UTC. These dropouts are attributed to an occultation of Jupiter that occurred during the pass. Juno's radio signal propagated through Jupiter's dense atmosphere, causing reductions in power from defocusing effects and refractive bending [10]. The dropout on 2023-250 from 12:38 to 12:51 UTC occurred for the same reason (Figure 8).

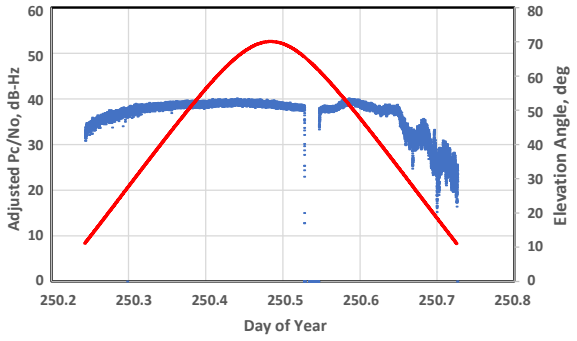

Figure 7. Adjusted P_C/N_0 (blue) and elevation angle (red) versus Day of Year for 2023-250.

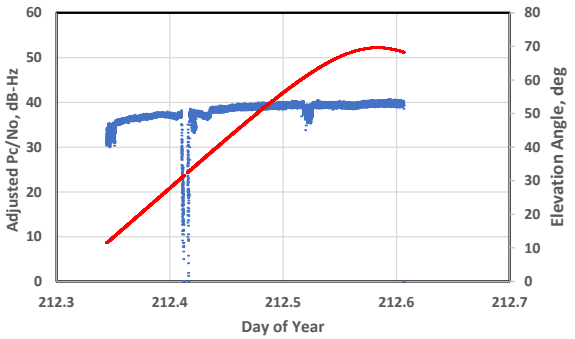

Figure 8. Adjusted P_C/N_0 (blue) and elevation angle (red) versus Day of Year for 2023-212.

2. Goldstone DSS-26 Ka-band Observations

This next section summarizes the statistical results of closed-loop receiver observations of Juno Ka-band carrier data acquired at DSS-26. Shown in Figure 9 below are the adjusted P_c/N_0 versus elevation angle for the Ka-band tracks in 2015, 2018, and 2019.

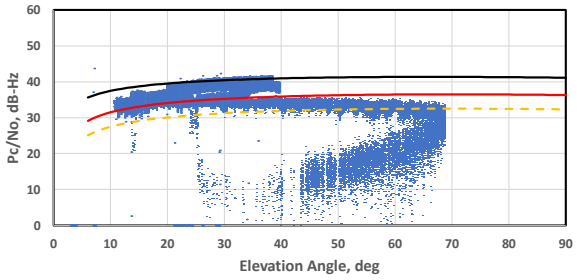

Figure 9. Ka-band Adjusted P_C/N_0 versus elevation angle for DSS-26 passes in 2015, 2018, and 2019. Also shown are the Favorable (black), Adverse (red), and Adverse – 4 dB (dashed yellow) link curves.

The adjusted P_c/N_0 versus elevation angle signatures in Figure 9 for years 2018 and 2019 appear nominal but we note an unusual signature in Adjusted P_c/N_0 for year 2015 (see Figure 10). Upon examination of the time series for this pass, which occurred on 2015/168–169, we see that the first portion of the pass prior to meridian transit (maximum elevation angle) appeared nominal although reduced in signal strength by several dB, whereas the latter portion of the pass (after meridian transmit) continued with a more significant excursion of reduced signal strength. This pass was a dedicated calibration track for the High Gain Antenna (HGA) pattern. Here, the spacecraft was commanded off-point away from the Earth in regular steps in order to measure the HGA beam pattern. Near the end of the track, the spacecraft was commanded to point the HGA boresight at Earth, thus increasing received signal strength back to nominal levels.

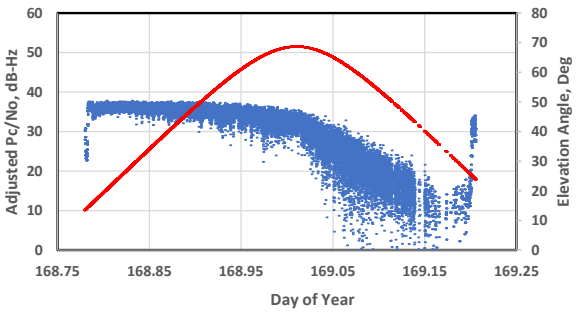

Figure 10. Adjusted P_C/N_0 (blue) and elevation angle (red) versus day of year for DSS-26 pass 2015-168/169.

B. Canberra

This section summarizes the statistical results of closed-loop receiver observations of Juno Ka-band carrier data acquired at Canberra, Australia.

Table 2 summarizes the Juno Ka-band carrier data that were acquired by the closed-loop receivers at the 34-m antennas at Canberra, Australia; DSS-34 (Table 2a), DSS-35 (Table 2b), DSS-36 (Table 2c) and the totals for all three stations (Table 2d). The table columns show the year of the observations, the total number of data points, the number of valid observations (displayed in the figures to follow) after removal of known "invalid" or "bad" points, number of data points lying above the Adverse – 4 dB curve and the percentage of valid data points lying above the Adverse – 4 dB curve. There were about 487 thousand total observations and about 484 thousand observations after removing those dealing with

Table 2. Summary of Juno Ka-band Carrier Observations Acquired at Canberra

Table 2a - Canberra DSS-34

Year	Number of Total Obs	Number of Valid Obs	Number Obs > Adv. – 4 dB	Percent > Adv. – 4 dB
2020	34,216	34,125	34,120	99.985
2021	33,748	33,689	33,680	99.973
2022	19,948	19,467	19,450	99.913
Total	**87,912**	**87,281**	**87,250**	**99.96**

Table 2b - Canberra DSS-35

Year	Number of Total Obs	Number of Valid Obs	Number Obs > Adv. – 4 dB	Percent > Adv. – 4 dB
2018	41,633	41,435	41,191	99.411
2019	99,552	99,552	99,510	99.958
2020	13,869	13,776	13,761	99.891
2021	87,784	87,610	85,958	98.114
2022	57,093	56,953	51,652	90.692
2023	61,247	61,016	57,557	94.331
Total	**361,178**	**360,342**	**349,629**	**97.03**

Table 2c - Canberra DSS-36

Year	Number of Total Obs	Number of Valid Obs	Number Obs > Adv. – 4 dB	Percent > Adv. – 4 dB
2020	21,250	20,121	20,103	99.911
2022	16,322	15,860	15,851	99.943
Total	**37,572**	**35,981**	**35,954**	**99.92**

Table 2d - Canberra Totals

Station	Number of Total Obs	Number of Valid Obs	Number Obs > Adv. – 4 dB	Percent > Adv. – 4 dB
DSS-34	87,912	87,281	87,250	99.964
DSS-35	361,178	360,342	349,629	97.027
DSS-36	37,572	35,981	35,954	99.925
Total	**486,662**	**483,604**	**472,833**	**97.77**

injected signals during calibrations (Table 2d). For the most part, the results appear nominal with about 98% of the valid observations lying above the "Adverse – 4 dB" curves. The valid observations are those that remain after removing known invalid points such as due to calibrations. The overall low ~97% of the data lying above the Adverse – 4 dB curve for DSS-35 are attributed to the lower percentages from years 2022 and 2023 (Table 2b).

1. Canberra DSS-34 Ka-band Observations

This section summarizes the statistical results of closed-loop receiver observations of Juno Ka-band carrier data acquired at DSS-34. Table 2a summarizes the observations where the results are nominal with about 99.96% of the valid observations lying above the "Adverse – 4 dB" curves. Figure 11 displays the individual adjusted P_c/N_0 data points from DSS-34 (in blue) for years 2020, 2021, and 2022. Also shown are the Favorable link curve (solid black), the Adverse link curve (solid red), and the 4 dB down from Adverse (dashed yellow). It should be noted that the data displayed in each of the years in Figure 11 are from single passes: 2020-206, 2021-105/106, and 2022-142/143. All of the data appear nominal and thus do not warrant any additional comment.

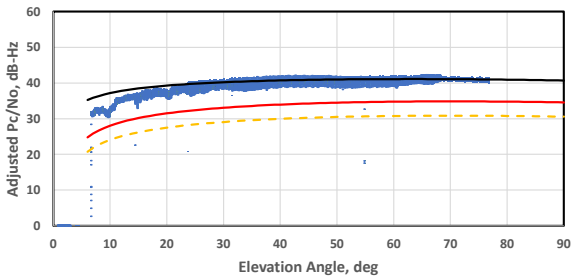

Figure 11. Adjusted Ka-band P_C/N_0 versus elevation angle (blue) from DSS-34 for years 2020, 2021, and 2022. Also shown are the Favorable (black), Adverse (red), and Adverse – 4 dB (dashed yellow) link curves.

2. Canberra DSS-35 Ka-band Observations

This section summarizes the statistical results of closed-loop receiver observations of Juno Ka-band carrier data acquired at DSS-35. Table 2b summarizes the observations where the results are nominal with about 97.0% of the valid observations lying above the "Adverse – 4 dB" curve.

Figure 12 displays the individual adjusted P_c/N_0 data (blue points) from DSS-35 (in blue) for passes conducted in years 2018, 2019, 2020, 2021, 2022, and 2023. Also shown are the Favorable link curve (solid black), the Adverse link curve (solid red), and the 4 dB down from Adverse (dashed yellow). As expected, the vast majority of the data points lie in between the Favorable and Adverse link curves, as well as the top of the envelope of the blue data points, essentially lining up against the Favorable link curve. Note that several "invalid" or "bad" data points are removed from the data sets for various reasons. Among these invalid points were those due to injected calibration signals prior to (i.e., during pre-cal time) or after (i.e., during post-cal time) the tracks.

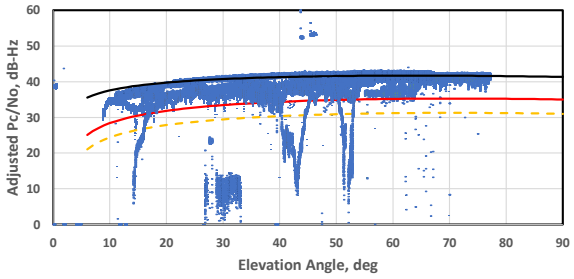

Figure 12. Adjusted Ka-band P_C/N_0 versus elevation angle (blue) from DSS-35 for years 2018, 2019, 2020, 2021, 2022, and 2023. Also shown are the Favorable (black), Adverse (red) and Adverse – 4 dB (dashed yellow) link curves.

The following plots display the times series of adjusted P_c/N_0 and elevation angle for some individual passes, where anomalies or significant degradation have been noted.

Figure 13 displays the time series of adjusted P_c/N_0 for DSS-35 pass 2018-181. Here the monopulse pointing system failed to calibrate due to an issue with the amplifier. The antenna was thus not pointed correctly and the issue with the amplifier had other not-entirely-understood (at the time) implications.

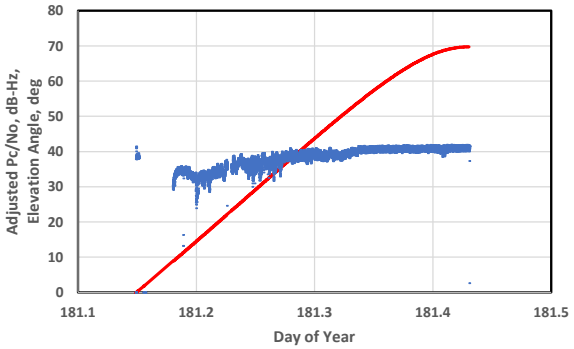

Figure 13. DSS-35 adjusted P_C/N_0 (blue) and elevation angle (red) versus Day of Year for 2018-181.

Figure 14 displays the time series of adjusted P_c/N_0 for DSS-35 pass 2018-197. There were some issues maintaining lock. The wind speed was fairly consistent at 10 km/hr from 08:00–11:00, after which the wind subsides.

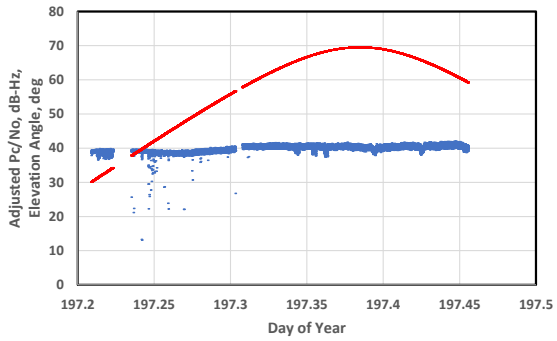

Figure 14. DSS-35 adjusted P_C/N_0 (blue) and elevation angle (red) versus Day of Year for 2018-197.

Figure 15 displays the time series of adjusted P_c/N_0 for DSS-35 pass 2020-313. The monopulse was not enabled due to operator error until 04:30 UTC (day 313.188), likely causing the reduction of signal strength during the beginning of the pass.

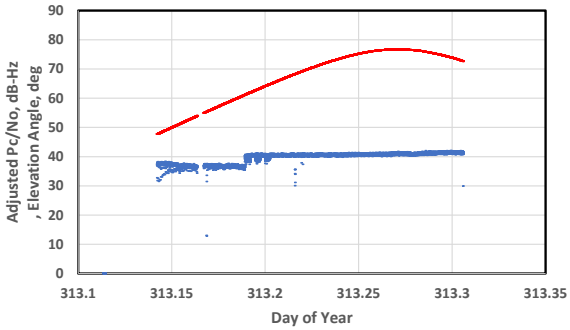

Figure 15. DSS-35 adjusted P_C/N_0 (blue) and elevation angle (red) versus Day of Year for 2020-313.

Figure 16 displays the time series of adjusted P_c/N_0 for DSS-35 pass 2021-138: This was an engineering demonstration that was in progress where the spacecraft transponder was purposely locked and unlocked several times throughout the track. Each time the transponder unlocked, the closed-loop receiver also dropped lock, which explains the reduced signal strength data points centered around the middle of the track (presumably occurring just after relocking).

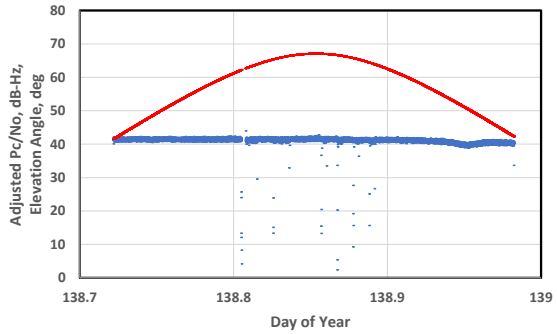

Figure 16. DSS-35 adjusted P_C/N_0 (blue) and elevation angle (red) versus Day of Year for 2021-138.

Figure 17 displays the time series of adjusted P_c/N_0 for DSS-35 pass 2021-142: This was another engineering demonstration where the antenna was manually forced off-point to examine open-loop receiver (OLR) tracking thresholds. Starting at 15:45 UTC (142.656 d on plot), pointing offsets of 50–80 millidegrees were implemented that resulted in a major degradation of Ka-band power (on the side lobe of the DSN antenna).

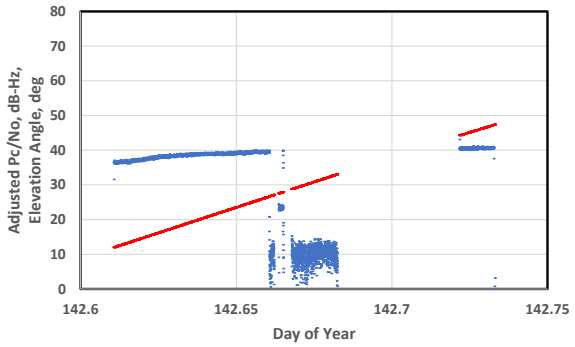

Figure 17. Adjusted P_C/N_0 (blue) and elevation angle (red) versus Day of Year for DSS-35 2021-142.

Figure 18 displays the time series of adjusted P_c/N_0 for DSS-35 pass 2022-055/056. The heavy rain that occurred over Canberra throughout the pass was responsible for the signal variations that are more pronounced near the end of the pass. The system noise temperature (SNT) was extremely high, exceeding 100 K at times. The X-band (8.4 GHz) link was also affected.

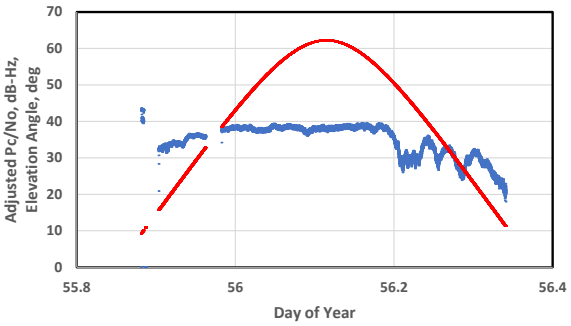

Figure 18. DSS-35 adjusted P_C/N_0 (blue) and elevation angle (red) versus Day of Year for 2022-055/056.

Figure 19 displays the time series of adjusted P_c/N_0 (blue) for DSS-35 pass 2023-022 along with elevation angle (red) and wind speed measurements (green) from a nearby weather sensor. The adjusted P_c/N_0 signal drop centered about day 22.17 illustrates the effects of being correlated with very high wind speeds that exceeded 40 km/hr, evidently taking the antenna off point. The signal drop centered around day 22.3 cannot be readily explained by the wind speed measurements which lie below 10 km/hr. The on-site rain gauge data for this date were not available.

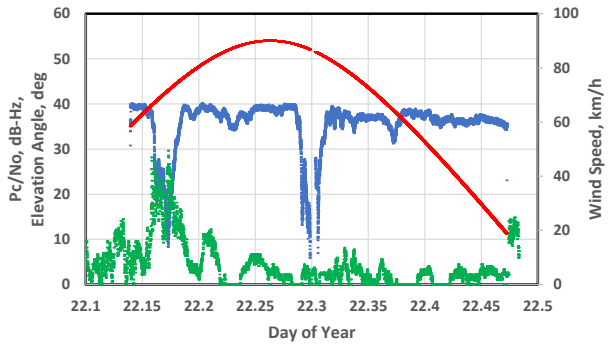

Figure 19. Adjusted P_C/N_0 (blue), elevation angle (red), and wind speed (green) versus Day of Year for DSS-35 on 2023-022.

Figure 20 displays the time series of adjusted P_c/N_0 for DSS-35 pass 2023-059/060. The large signal reduction at the end of pass is attributed to very heavy rain over Canberra resulting in severely degraded data from 08:40–09:10 UTC. The signal variation near and before timestamp ~60.1 d may be due to issues with the frequency predicts as the monopulse was not enabled until later in the pass.

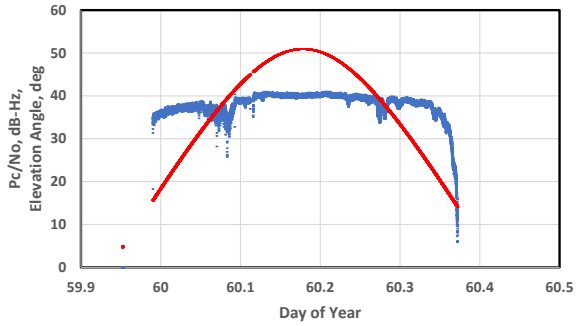

Figure 20. Adjusted P_C/N_0 (blue) and elevation angle (red) versus Day of Year for DSS-35 on 2023-059/060.

3. Canberra DSS-36 Ka-band Observations

This section summarizes the statistical results of closed-loop receiver observations of Juno Ka-band carrier data acquired at DSS-36. Table 2c summarizes the observations. The results are nominal with about 99.92% of the valid observations lying above the "Adverse – 4 dB" curves. The valid observations are those that remain after removing known invalid points such as those due to calibrations.

Figure 21 displays the individual adjusted P_c/N_0 data points from DSS-36 (in blue) for years 2020 and 2022. Also shown are the Favorable link curve (solid black), the Adverse link curve (solid red), and the 4 dB down from Adverse (dashed yellow). It should be noted that the data displayed in the DSS-36 plots are from two single passes in 2020 and from one single pass in 2022. All of the data appear nominal and no additional comment is warranted.

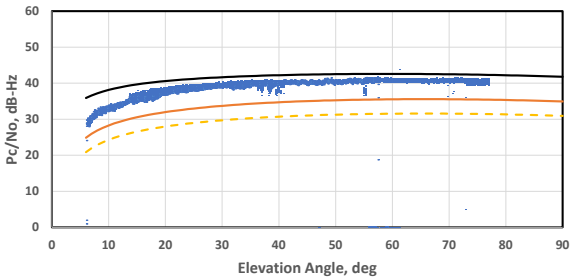

Figure 21. Adjusted Ka-band P_C/N_0 versus elevation angle (blue) from DSS-36 for years 2020 and 2022. Also shown are the Favorable (black), Adverse (red), and Adverse – 4 dB (dashed yellow) link curves.

C. Madrid

Table 3 summarizes the Juno Ka-band carrier data that were acquired by the closed-loop receivers at the 34-m antennas located at Madrid, Spain (3a) DSS-53, (3b) DSS-54, (3c) DSS-55, (3d) DSS-56 and (3e) Madrid totals, showing the year of the observations, the total number of data points, the number of valid observations (displayed in the figures after removal of known "invalid" or "bad" points), number of data points lying above the Adverse – 4 dB curve and the percentage of valid data points lying above the Adverse – 4 dB curve. We note that overall lower ~96.62% of the data lying above the Adverse – 4 dB curve for DSS-53 (Table 3a), are due to the very low 91.7% percentage from year 2022; details are provided in Table 3.

Table 3 – Summary of Juno Ka-band Carrier Observations Acquired at Madrid

Table 3a - Madrid DSS-53

Year	Number of Total Obs	Number of Valid Obs	Number Obs > Adv. – 4 dB	Percent > Adv. – 4 dB
2021	12,463	12,405	12,396	99.927
2022	83,497	83,379	76,469	91.713
2023	113,027	112,795	112,660	99.880
Total	**208,987**	**208,579**	**201,525**	**96.62**

Table 3b - Madrid DSS-54

Year	Number of Total Obs	Number of Valid Obs	Number Obs > Adv. – 4 dB	Percent > Adv. – 4 dB
2020	4,329	4,317	4,313	99.907
Total	**4,329**	**4,317**	**4,313**	**99.91**

Table 3c - Madrid DSS-55

Year	Number of Total Obs	Number of Valid Obs	Number Obs > Adv. – 4 dB	Percent > Adv. – 4 dB
2015	8,128	8,017	8,013	99.950
2016	40,139	39,657	39,639	99.955
2021	86,905	86,731	86,699	99.963
2022	133,338	133,048	132,961	99.935
Total	**268,510**	**267,453**	**267,312**	**99.95**

Table 3d - Madrid DSS-56

Year	Number of Total Obs	Number of alid Obs	Number Obs > Adv. – 4 dB	Percent > Adv. – 4 dB
2020	11,131	11,010	10,938	99.346
2021	9,079	9,021	9,013	99.911
2023	28,280	28,222	28,210	99.957
Total	**48,490**	**48,253**	**48,161**	**99.81**

Table 3e - Madrid Totals

Station	Number of Total Obs	Number of Valid Obs	Number Obs > Adv. – 4 dB	Percent > Adv. – 4 dB
DSS-53	208,987	208,579	201,525	96.618
DSS-54	4,329	4,317	4,313	99.907
DSS-55	268,510	267,453	267,312	99.947
DSS-56	48,490	48,253	48,161	99.809
Total	**530,316**	**528,602**	**521,311**	**98.62**

1. Madrid DSS-53 Ka-band Observations

Figure 22 displays the adjusted Ka-band P_c/N_0 versus elevation angle (blue) from DSS-53 for the three years in which the antenna was used to acquire data: 2021 (one pass 2021-300), 2022 (two passes 2022-143 and 2022-348), and 2023 (three passes: 2023-199, 2023-207, 2023-212). Upon inspection, years 2021 and 2023 appear nominal while 2022 shows a pass with a significant rain event (2022-348). Also shown in Figure 22 are the Favorable (black curve), Adverse (red curve), and Adverse – 4 dB (dashed yellow) link curves.

Figure 23 displays the adjusted P_c/N_0, elevation angle, and rain rate as a function of time for pass 2022-348, where the rain event occurs at the start of the pass. Upon inspection, one can see that the fades at the start of the pass are well correlated with non-zero rainfall data from the on-site rain gauge. One can infer that the deepest dive and apparent loss of signal on ~348.7 d (16:44 UTC) lines up well with the maximum recorded rain rate of 90 mm/h at that time.

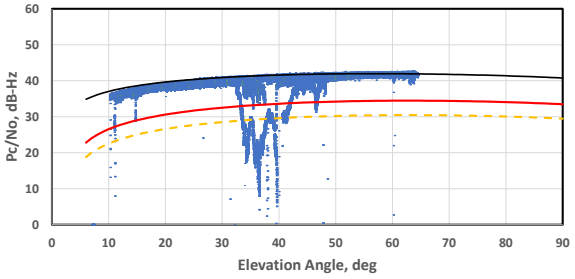

Figure 22. Adjusted Ka-band P_c/N_0 versus elevation angle (blue) from DSS-53 for years 2021, 2022, and 2023. Also shown are the Favorable (black), Adverse (red), and Adverse – 4 dB (dashed yellow) link curves.

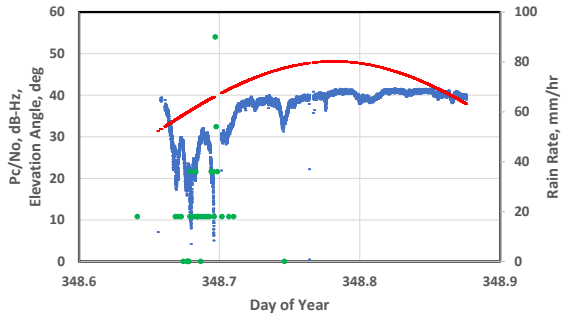

Figure 23. Adjusted P_C/N_0 versus time (blue), elevation angle (red), and rain rate (green) for DSS-53 pass 2022-348

2. Madrid DSS-54, DSS-55, and DSS-56 Ka-band Observations

Figure 24 displays the adjusted P_c/N_0 versus elevation angle data for DSS-54 in 2020 (one pass 2020-259), DSS-55 for 2015 (one pass 2015-325), DSS-55 for 2016 (two passes: 2016-226, 2016-240), DSS-55 for 2021 (four passes: 2021-052, 2021-159, 2021-246, 2021-289), DSS-55 for 2022 (five passes: 2022-012, 2022-099, 2022-186, 2022-272, and 2022-310), DSS-56 in 2020 (one pass 2020-280), DSS-56 in 2021 (one pass 2021-202), and DSS-56 in 2023 (one pass: 2023-202). The vast majority of the data appear nominal and thus no additional comment is warranted.

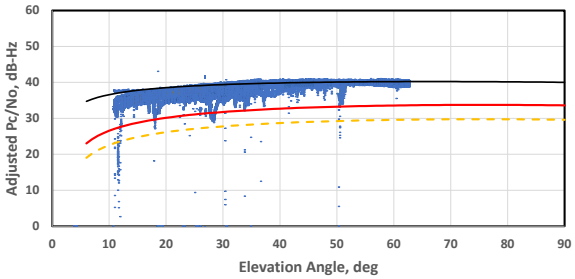

Figure 24. Adjusted P_C/N_0 versus elevation angle data for DSS-54 in 2020, DSS-55 for 2015, DSS-55 in 2016, DSS-55 in 2021, DSS-55 in 2022, DSS-56 in 2020, DSS-56 in 2021, and DSS-56 in 2023. Also shown are the Favorable (black), Adverse (red), and Adverse – 4 dB (dashed yellow) link curves.

III. Discussion

Table 4 displays the overall summary of the statistics by DSN complex for the case of Juno Ka-band. A total of 3,706,427 valid observations from all three complexes were examined, of which 3,642,950 lied above the "Adverse – 4 dB" link curve, resulting in an overall 98.3% rate.

Table 4 – Summary of Juno Ka-band Carrier Observations by DSN Complex

	Juno Ka-band Totals			
Complex	Number of Total Obs	Number of Valid Obs	Number Obs > Adv. – 4 dB	Percent > Adv. – 4 dB
Goldstone	2,736,055	2,694,221	2,648,806	98.314
Canberra	486,662	483,604	472,833	97.773
Madrid	530,316	528,602	521,311	98.621
Total	**3,753,033**	**3,706,427**	**3,642,950**	**98.29**

Table 5 summarizes the overall statistics of all Ka-band observations acquired at each of the three DSN complexes involving the four deep-space Ka-band downlink missions (Cassini, Kepler, MRO, and Juno) where closed-loop carrier observations were available, delivered, and examined. We see that Goldstone achieved 98% (Table 5a), Madrid achieved 96% (Table 5b) and Canberra achieved 98% (Table 5c) of the observations lying above the Adverse – 4 dB curve. The Juno rates do not appear to be very much different than those from the other Ka-band missions, lying near the 98% to 99% level. The reasons that some observations may lie below the "Adverse – 4 dB" curve include weather-induced effects such as those due to rain and wind, procedural and equipment issues, and some non-standard spacecraft maneuvers that were left in the delivered data sets (for example occultation or antenna/equipment calibrations). In some cases, some data were excluded, such as when Cassini was under thruster control which provided usable X-band data but severely degraded Ka-band data during large signal strength variations during dead-banding swings [1]. Thus, a total of 6,512,426 valid observations from all three complexes and all four Ka-band missions were examined, of which 6,351,572 lay above the "Adverse – 4 dB" link curve, resulting in an overall 97.6% rate.

Future work involves performing the analysis on Parker Solar Probe Ka-band data and folding the resulting statistics into this database.

Table 5. Summary of Ka-band Carrier Observations

Table 5a - Goldstone

	Number of Obs	Number Obs > Adv. – 4 dB	Percent > Adv. – 4 dB	Notes
Cassini	730,922	715,738	97.92	Ref. [1]
Kepler	131,108	124,889	95.26	Ref. [2]
MRO	112,974	110,808	98.08	Ref. [3]
Juno	2,694,221	2,648,806	98.31	This Study
Total	**3,669,225**	**3,600,241**	**98.12**	

Table 5b - Madrid

	Number of Obs	Number Obs > Adv. – 4 dB	Percent > Adv. – 4 dB	Notes
Cassini	832,745	785,738	94.36	Ref. [1]
Kepler	142,101	139,751	98.35	Ref. [2]
MRO	121,747	116,108	95.37	Ref. [3]
Juno	528,602	521,311	98.62	This Study
Total	**1,625,195**	**1,562,908**	**96.17**	

Table 5c - Canberra

	Number of Obs	Number Obs > Adv. – 4 dB	Percent > Adv. – 4 dB	Notes
Cassini	527,328	512,100	97.11	Ref. [1]
Kepler	86,793	83,362	96.05	Ref. [2]
MRO	120,281	120,128	99.87	Ref. [3]
Juno	483,604	472,833	97.77	This Study
Total	**1,218,006**	**1,188,423**	**97.57**	

IV. Conclusion

Ka-band downlink carrier signal-to-noise density ratio from Juno were characterized against a modeled link budget in Favorable and Adverse conditions defined by Earth atmospheric weather. These results were sorted by year of the data collection, DSN antenna, and DSN complex. At the Goldstone complex, where a majority of Juno data were collected, 98.31% of Ka-band P_c/N_0 measurements lie above an Adverse – 4dB link model. Canberra and Madrid had 97.77% and 98.62% of Ka-band P_c/N_0 measurements, respectively, lie above the Adverse – 4dB link model. These Juno Ka-band statistics are combined with those derived from previous studies involving the Cassini, Kepler and, MRO spacecraft Ka-band downlinks. Such statistics are useful to future missions that may be considering incorporating a Ka-band link on their spacecraft, to assist in their design and link budget modeling.

Acknowledgments

We would like to thank Steve Lichten and Douglas Abraham of the SCaN Program System Engineering for providing support. We would also like to thank Dennis Lee for his thorough review of this manuscript.

References

[1] D. D. Morabito, D. Kahan, K. Oudrhiri, and C.-A. Lee, "Cassini downlink ka-band carrier signal analysis. *The Interplanetary Network Progress Report,* vol. 42-208, Jet Propulsion Laboratory, Pasadena, California, February 15, 2017. https://ipnpr.jpl.nasa.gov/progress_report/42-208/208B.pdf

[2] D. D. Morabito, "Deep-space ka-band flight experience." *The Interplanetary Network Progress Report,* vol. 42-211, Jet Propulsion Laboratory, Pasadena, California, November 15, 2017. https://ipnpr.jpl.nasa.gov/progress_report/42-211/211B.pdf

[3] D. D. Morabito, "Mars Reconnaissance Orbiter ka-band carrier signal analysis." *The Interplanetary Network Progress Report,* vol. 42-214, Jet Propulsion Laboratory, Pasadena, California, pp. 1–16, August 15, 2018. https://ipnpr.jpl.nasa.gov/progress_report/42-214/42-214B.pdf

[4] D. D. Morabito and D. Heckman, "Lunar Reconnaissance Orbiter k-band (26 GHz) signal analysis: initial study results." *The Interplanetary Network Progress Report,* vol. 42-211, Jet Propulsion Laboratory, Pasadena, California, November 15, 2017. https://ipnpr.jpl.nasa.gov/progress_report/42-211/211A.pdf

[5] D. D. Morabito and D. Heckman, "Lunar Reconnaissance Orbiter k-band (26 GHz) signal analysis: updated study results." *The Interplanetary Network Progress Report,* vol. 42-222, Jet Propulsion Laboratory, Pasadena, California, pp. 1–15, August 15, 2020. https://ipnpr.jpl.nasa.gov/progress_report/42-222/42-222B.pdf

[6] D. D. Morabito, "Ka-band estimated and observed frame error analysis." *The Interplanetary Network Progress Report,* vol. 42-216, Jet Propulsion Laboratory, Pasadena, California, pp. 1–16, February 15, 2019. https://ipnpr.jpl.nasa.gov/progress_report/42-216/42-216B.pdf

[7] S. D. Slobin, "Atmospheric and environmental effects." In *DSMS Telecommunications Link Design Handbook,* Doc. 810-005, Module 105, Rev. E, Jet Propulsion Laboratory, California Institute of Technology, Pasadena, California, 2015. https://deepspace.jpl.nasa.gov/dsndocs/810-005/105/105E.pdf

[8] S. D. Slobin, "34-m BWG stations telecommunications interfaces." In *DSMS Telecommunications Link Design Handbook,* Doc. 810-005, Module 104, Rev. O, Jet Propulsion Laboratory, California Institute of Technology, Pasadena, California, 2022. https://deepspace.jpl.nasa.gov/dsndocs/810-005/104/104O.pdf

[9] M. A. Gudim, W. Gawronski, W. J. Hurd, P. R. Brown, and D. M. Strain, "Design and performance of the monopulse pointing system of the DSN 34-meter beam-waveguide antennas." In *Telecommunications and Mission Operations Progress Report,* vol. 42, no. 138, 1999.

[10] D. Buccino, M. Parisi, D. Kahan, H. Wilson, O. Yang, E. Barbinis, et al., and R. S. Park, "Planning and execution of Juno radio occultation experiments at Jupiter." In *2023 IEEE Aerospace Conference*, pp. 1–10, March 2023, IEEE.